Available online at BCREC Website: http://bcrec.undip.ac.id

Bulletin of Chemical Reaction Engineering & Catalysis, 8 (2), 2013, 145-153

Research Article

Visible Light Induced Photocatalytic Activity of Polyaniline Modified TiO_2 and Clay-TiO_2 Composites

K.P. Sandhya[a], Suja Haridas[b], S. Sugunan[a]*

[a] *Department of Applied Chemistry, Cochin University of Science and Technology, Cochin-682022, Kerala, India*

[b] *Department of Chemistry, N.S.S. College, Nenmara, Palakkad, India*

Received: 15th May 2013; Revised: 1st September 2013; Accepted: 3rd October 2013

Abstract

Sonochemical synthesis of Titania, Titania-Polyaniline, and Clay-Titania-Polyaniline composites were carried out. The composite systems were characterized by various physico-chemical techniques. Photocatalytic activity was tested selecting some common dyes as substrates. Composites exhibited higher activity for the degradation of dyes under visible light in most of the cases.

Keywords: titania-polyaniline; clay-titania-polyaniline; dye degradation

How to Cite: Sandhya, K.P., Haridas, S., Sugunan, S. (2013). Visible Light Induced Photocatalytic Activity of Polyaniline Modified TiO_2 and Clay-TiO_2 Composites. *Bulletin of Chemical Reaction Engineering & Catalysis*, 8(2): 145-153. (doi:10.9767/bcrec.8.2.4949.145-153)

Permalink/DOI: http://dx.doi.org/10.9767/bcrec.8.2.4949.145-153

1. Introduction

Organic dyes widely used in textile and food industries represent an important source of environmental contamination. Most of dyes are toxic on aquatic creatures and have carcinogenic effects on humans [1,2]. Different techniques such as adsorption, oxidation, reduction, electrochemical and membrane filtration have been applied for the removal of these pollutants from the industrial effluents [3,4]. Research activities in the domain of photocatalysis have acquired strong momentum in the past few years. It is now regarded as a clean and attractive, low temperature, on-energy intensive approach for waste water treatment since it achieves complete mineralization of toxic wastes. Semiconductors have been the most preferred photocatalysts due to the narrow band gap between valence and conduction bands. Semiconductor photocatalysis has been another emerging area with wide applications in solving environmental issues due to their suitable band gap energy to catalyze a wide variety of organic degradation reactions [5,6]. TiO_2 has been the most opted one in this regard due to its biological and chemical inertness, stability against photocorrosion and chemical corrosion, cost effectiveness etc. [7-9]. Photoexcitation of titania by light of suitable energy results in the formation of electron-hole pairs, which by migration to the surface react with the substrate through a redox process. However, the utilization efficiency of solar light is limited severely by the wide band gap of TiO_2 (3.2 eV). Hence, much effort has been directed towards improving the utilization of solar light by extending the photoresponse of TiO_2 to the visible region. These include metal ion doping [9], non-metal doping [10-12], noble metal deposition [13], narrow band-gap semiconductor coupling [14]

* Corresponding Author.
E-mail: ssg@cusat.ac.in (S. Sugunan),
Tel: +91-484-2575804 , Fax: +91-484-2577595

and dye sensitization [15,16].

Delocalized conjugated structures have been proven to arouse a rapid photoinduced charge separation and decrease in the charge recombination rate in electron-transfer processes [17,18]. Conducting polymers, such as polyaniline (PANI), polythiophene, polypyrrole, and their derivatives, have been reported as promising sensitizers to extend the spectral response of TiO_2 to visible region [19-21]. As a typical conducting polymer, polyaniline (PANI) has unique electrical, optical and photoelectric properties. Most importantly, it is cheaper than other conducting polymers. Zhu *et al.* reported the photocatalytic degradation of methyl orange using Polythiophene/Titanium dioxide composites [22]. Gu *et al.* reported the photocatalytic degradation of Rhodamine B using a novel TiO_2-Polyaniline composite [23]. It was found that the prepared composites found to be very efficient photocatalyst under visible light irradiation [23]. Inert supports, like clay, mesoporous silicates, activated carbon, carbon nanotubes, etc., were used to improve the structural properties of titania. These materials also act as good adsorbents and facilitate pollutant elimination. The enhanced activity may be due to a combined effect of the high adsorbing capacities of the support together with the photo catalytic activity of TiO_2. Low temperature synthesis of TiO_2 pillared montmorillonite was undertaken by Zhang *et al.* [24], while its photocatalytic efficiency for the degradation of Acid Orange G was examined.

The present study attempts to utilize the advantages of the conducting polymers as well as the support materials in a single system. Montmorillonite was selected as support in the present study due to its unique properties. We make use of the adsorption ability of the clay montmorillonite. Here we report the preparation of polyaniline-TiO_2 and Clay-TiO_2 polyaniline composites by '*in situ*' chemical oxidative polymerization of aniline. The prepared systems were scanned for their visible light sensitivity taking some common dyes as substrates.

2. Experimentals

2.1. Reagents and Materials

Titanium Isopropoxide (Sigma Aldrich), Glacial aceticacid (MERCK), Distilledwater, Aniline(SDFineChemicals), Ammoniumperoxodisulphate(MERCK), Con.HCl (SDFCL), Montmorillonite K-10 (Sigma Aldrich), Acid blue 25 (Sigma Aldrich), Acid Orange-7 (Sigma Aldrich), Methylene Blue (SRL**).**

2.2. Preparation of Catalysts

2.2.1. Pure TiO_2

Titanium isopropoxide and acetic acid in a volume ratio 1:2 was taken in a beaker and magnetically stirred with dropwise addition of distilled water from a dropping funnel. The clear sol obtained was sonicated for 3 hours, transferred to an autoclave and kept overnight at 110 °C. The resultant solution after solvent evaporation was dried in an air oven at 110 °C followed by calcinations at 500 °C for 5 hours.

2.2.2. TiO_2-PANI (TP)

Ammonium peroxodisulphate solution (12.5 g in 100 ml) was added drop wise to a mixture of 2.5 g TiO_2 in 100 ml 1 M HCl solution and 5 ml of distilled aniline kept in an ice bath under constant stirring. The mixture after sonication for about 3 hours was transferred to an autoclave and kept overnight at 110°C. It was filtered, washed with water and acetone to remove unreacted aniline, and dried in an oven at 110 °C.

2.2.3. Clay-TiO_2-PANI (CTP)

Montmorillonite (K-10) after dispersion in distilled water through sonication was mixed with the titania sol (5:1 ratio). The mixture was sonicated for 3 hours, transferred into an autoclave kept overnight at 110 °C, filtered, washed with water, and dried at 110 °C overnight. The resulted powder was calcined at 500 °C for about 5 hours. The 5 g of the Clay-TiO_2 composite was sonicated (3 hrs) with 100 ml of 1 M HCl and 5 ml of aniline in an ice bath followed by dropwise addition of 100 ml of ammonium peroxodisulphate solution. The resultant mixture was transferred into an autoclave placed in an oven at 110 °C for overnight, filtered, washed with water and acetone, and dried at 110 °C.

2.3. Characterization

XRD patterns were recorded in Bruker AXS D8 Advance X-Ray Diffractometer using Ni filtered Cu K α radiation (λ=1.5406 Å) in the range 5- 70° at a scan rate 2°/min. The IR spectra of the samples were recorded using Thermo NICOLET 380 FTIR Spectrometer by means of KBr pellet procedure. Spectra were taken in the transmission mode and the spectra were taken under atmospheric pressure and room temperature. Absorbance Measurements as well as onset absorption were taken in a UV-Vis. Double beam UVD-3500, labomed, Inc Spectrophotometer. The scanning electron micrographs of the samples were taken using JEOL

Model JSM-6390LV scanning electron microscope with a resolution of 1.38 eV. The powdered samples were dusted on a double sided carbon tape, placed on a metal stub and was coated with a layer of gold to minimize charge effects.

Determination of surface area of the samples was achieved in a Micromeritics Tristar 3000 surface area and porosity analyzer. Prior to the measurements the samples were degassed at 110 °C for 6 h. TG/DTG analysis was done on a Perkin Elmer Pyris Diamond thermo gravimetric/differential thermal analyzer instrument under nitrogen atmosphere at a heating rate of 5-10 °/min from room temperature to 1000 °C.

The electrical conductivity was measured at room temperature using a standard Four Point Probe technique. The thickness of the pellets was measured by using a micrometer. The conductivity was calculated using the following equation:

$$\sigma = I \ln 2 / V\pi t \quad (1)$$

where σ =conductivity, I=current in Ampere, V= voltage in Volts and t =thickness of the pellet in cm [25].

2.4 Reactivity Studies

Photocatalytic activities of the prepared systems were scanned using Oriel Uniform illuminator (Newport Model 66901). For a typical reaction, 10 ml of 10^{-4} M dye solution was sonicated with the required amount of catalyst for 15 minutes to achieve equilibration and then exposed to white light with continuous stirring. At required intervals, the catalyst was removed by centrifugation and the residual concentration of the dye was monitored by UV absorbance method (Chemito, UV-Visible Spectrophotometer, and Spectroscan UV2600 with lamp intensity 150 W). Three types of dyes were used in the present study, i.e. Acid blue-25 (anionic dye), Methylene blue (cationic dye), and Acid orange-7 (azo dye).

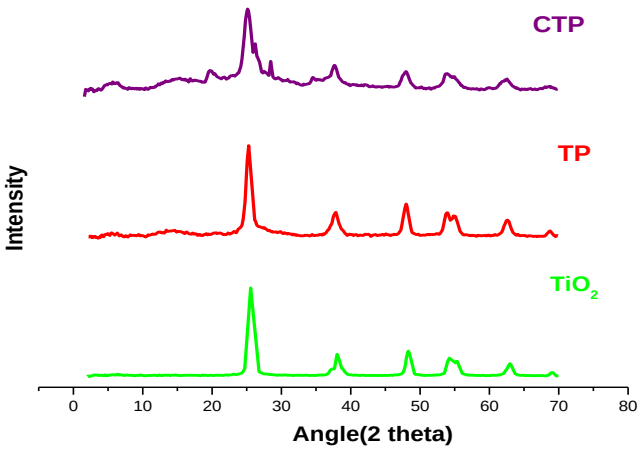

Figure 1. XRD spectra of the prepared samples

3. Results and Discussion

XRD patterns of the various samples are listed in Figure 1. Pure Titania showed the presence of only the photo catalytically active anatase phase 2θ = 25.5 (101) plane, 38 (004) plane, 48.3 (200) plane, 54 (105) plane, 55.2 (211) plane, 63 (204) plane, 68.9 (116) plane (JCPDS 21-1272). No characteristic peaks of rutile or brookite phase were observed indicating the high purity of the system. Pure PANI shows the Bragg peaks at 2θ = 9.4, 14.0, 15.7, 16.9, 26.5 and 27.4. It also shows two broad peaks centered at 2θ=20.8, 25.4, that are ascribed to the periodicity parallel and perpendicular to the polymer chain which indicate that pure PANI was in semi crystalline phases. In the case of Titania-PANI composite, the characteristic peaks of anatase phase with a slight lowering of intensity, whereas those of PANI disappeared or became weaker. This suggests that the addition of TiO_2 hampers the crystallization of the PANI molecular chain. When PANI is adsorbed onto the surface of TiO_2, the molecular chain of adsorbed PANI is tethered and the degree of crystallinity decreases [26]. PANI incorporation had no significant effect on the crystallization and phase characteristics of TiO_2. Clay-Titania Polyaniline nanocomposites also displayed peaks corresponding to anatase phase. Peaks corresponding to clay were observed with low intensity due to its highly amorphous nature. The crystallite size is calculated using Sherrer's equation and the values obtained are given in Table1. Upon polyaniline incorporation the crystallite size of TiO_2 and Clay TiO_2 was found to be decreased. Representative scanning electron micrographs (SEM) are presented in Figure 2. The SEM photographs indicate random dispersion of the TiO_2 and polyaniline in clay.

IR spectra of pure TiO_2 and polyaniline along with the composites were taken (Figure 3). Pure TiO_2 shows peaks around 456, 1623, 3441 cm^{-1}

Table 1. Crystallite size of the Prepared Samples

Sample name	Crystallite Size (nm)
TiO_2	12.4
TP	10.1
CTP	9.5

which may be attributed to the Ti-O-Ti stretching O-H bending, and O-H stretching respectively. Peaks for pure polyaniline appears at around 503 cm^{-1} (C-H out of plane bending vibration), 808 cm^{-1} (para substituted aromatic rings), 1133 cm^{-1} (C-H in plane bending) and 1294 cm^{-1} (C-N stretching). Two bands in the range 1450-1600 cm^{-1} can be assigned to the nonsymmetric C_6 ring stretching modes. Higher frequency band has higher contribution from quinoid ring and lower one from benzenoid ring. Peaks around 3795 cm^{-1} corresponds to N-H stretching whereas aromatic C-H stretching results in a band in the range 3000-2500 cm^{-1} [27].

PANI-TiO_2 composites are found to retain almost all the peaks of PANI and TiO_2. PANI is believed to undergo polymerization on the surface of TiO_2 [28]. Peaks at 1645 cm^{-1} (bending mode of water) and 3448 cm^{-1} (stretching mode of water) suggests the presence of water even after calcination. This is quite important since surface hydroxyl groups provide higher capacity for oxygen adsorption which is essential for the photocatalytic activity of anatase [29]. Clay-TiO_2-PANI composites also showed similar pattern. In addition, a band around 1115 cm^{-1} appeared due to the Si-O-Si stretching of clay skeletal structure.

The TG-DTG analysis enabled the evaluation of thermal stability of the systems (Figure 4). DTG pattern of pure TiO_2 shows a two stage decomposition pattern. A small weight loss around 100-200 °C, may be due to the removal of adsorbed water in the gel while the second one around 350 °C may be

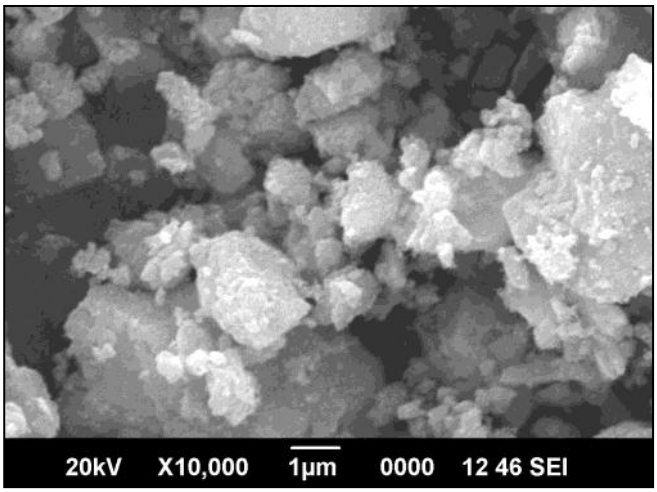

TiO_2

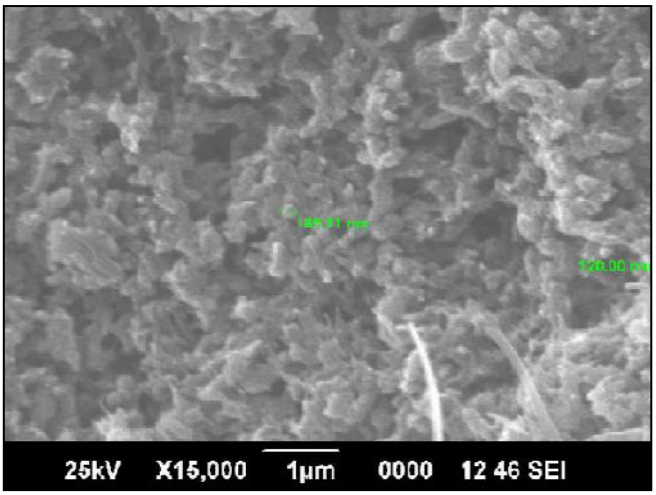

PANI

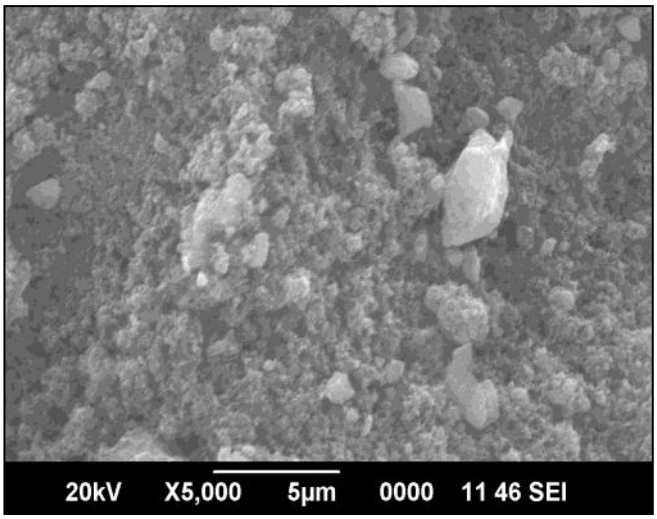

TiO_2-PANI

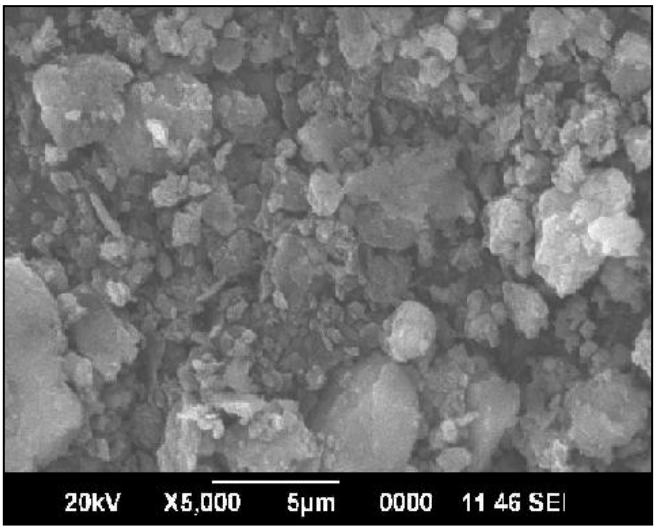

Clay- TiO_2-PANI

Figure 2. SEM images of prepared samples

attributed to the formation of TiO_2 by removal of strongly bound water and the surface hydroxyl groups along with the organic residue [30]. In the case of PANI, the first weight loss around 100 °C is attributed to the loss of water, the second weight loss (200-300 °C) to the loss of dopant HCl [31] and the third one may be due to the breakage of polymer backbone. TP shows a DTG pattern similar to that of pure PANI indicating a similar sequence of decomposition. However, for clay composites the DTG pattern was found to be rather broad without a major weight loss indicating higher thermal stability.

UV-Vis. diffuse reflectance spectrum of representative samples is sketched in Figure 5. Pure titania shows a sharp reflection peak at around 380 nm. In the case of the PANI doped systems, the pattern becomes broad with considerable absorption in the UV and visible region. This marked shifting of photoresponse indicates the prepared

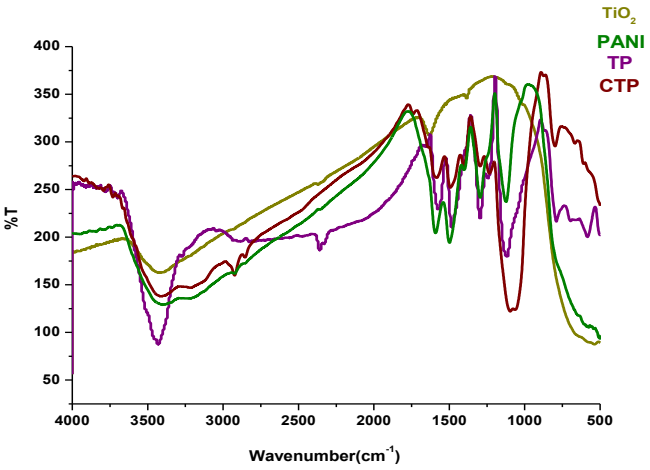

Figure 3. FT-IR Spectra of prepared Samples

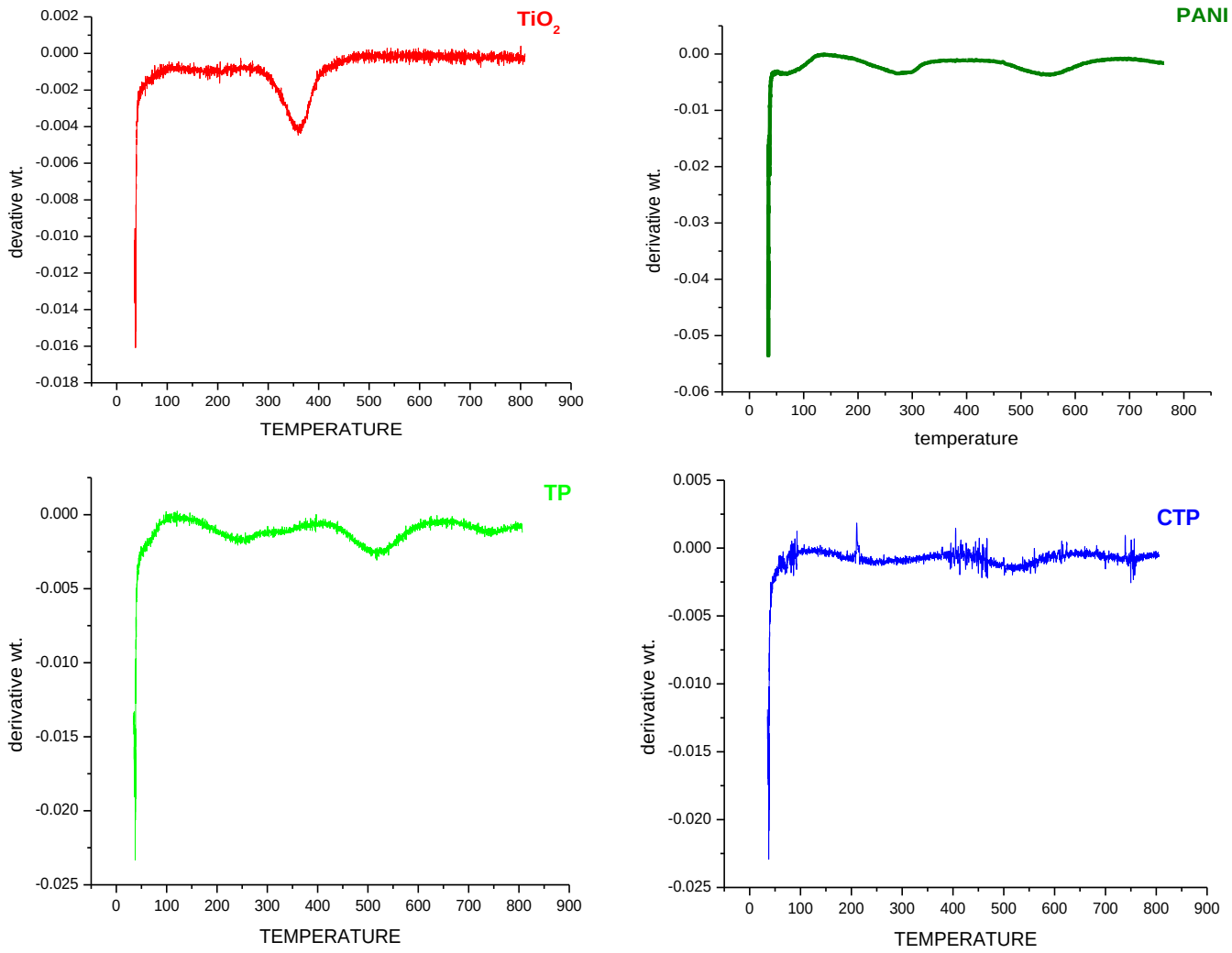

Figure 4. Differential thermogravimetric plots of the prepared samples

systems may be a good photocatalyst under visible light irradiation.

Surface area values as determined from the analysis is shown in Table 2. It was found that incorporation of polyaniline has a little impact on the surface area of the TP composites. In the case of Clay composites the surface area increases even after doping with TiO_2 and PANI. This may be to the delamination of clay layers upon composite formation.

The conductivity values measured by a four probe method are given in Table 3. A drastic reduction in conductivity was observed in the case of TP systems. Incorporation of clays resulted in a further lowering of conductivity. Irrespective of the type of composites a typical ohmic conductance pattern was observed and a representative graph is shown in Figure 6.

4. Reactivity Studies

The prepared catalysts were tested for their photocatalytic activity by selecting three common dyes belonging to different categories and the results are tabulated Table 4. Acid Blue-25 is a sulfonated anionic and Acid Orange-7 is a sulfonated azo dye. Sulfonated dyes undergo chemical interactions with the charged backbone of PANI leading to significant adsorption of the dye. This selective adsorption of dyes by PANI promises a green method for the removal of sulfonated organics from waste water. Sulfonated dyes in their aqueous solution exist in the anionic form. The $-SO_3^-$ group on the dye could lead to chemical interaction with positively charged backbone of PANI emeraldine salt. This will lead to the adsorption of various sulfonated dyes on the emeraldine salt of PANI. The adsorbed dye species are then degraded by hydroxyl and super oxide radicals.

In the case of Acid Blue-25, pure titania shows 56% degradation upon visible light irradiation. But on forming composite with PANI the extent of degradation shows a dramatic increase. With an increase in the amount of PANI in the composite, the extent of degradation first shows a sharp decrease and thereafter shows a regular increase. This indicates that the activity is strongly dependent on the concentration of PANI in the composite as well as the interaction between TiO_2 and PANI. High activity may be due to the strong interaction

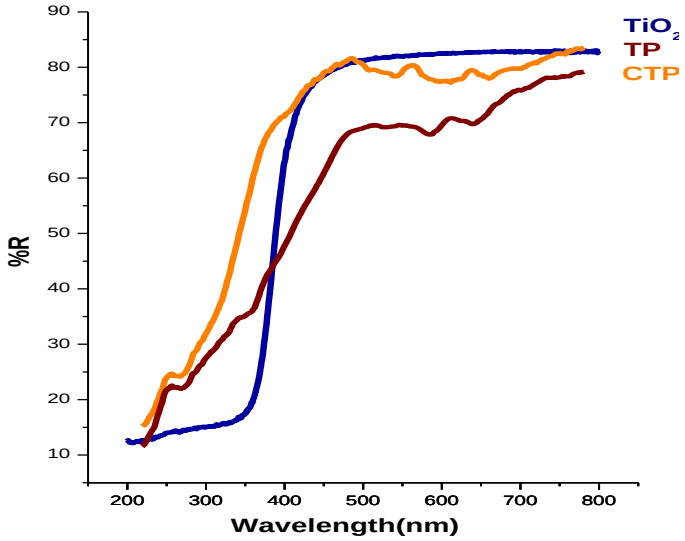

Figure 5. Diffuse reflectance spectra of the samples

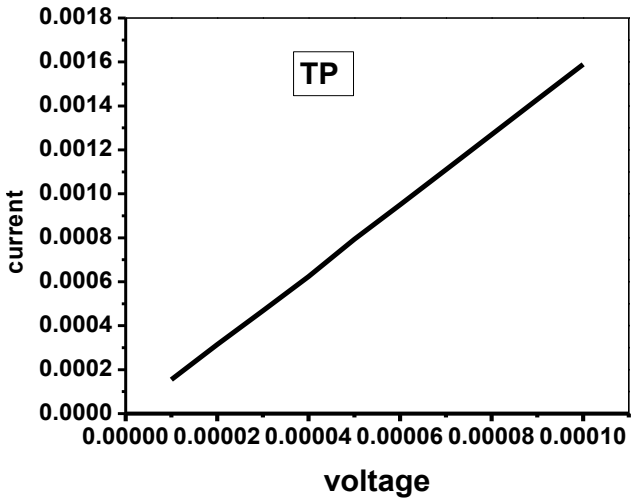

Figure 6. Representative V-I plots obtained from conductivity measurements

Table 2. Surface area of the samples

Sample name	BET Surface Area (m^2/g)
TiO_2	80.5
TP	76. 7
Clay	190
CTP	206.2

Table 3. Conductivity values of composites.

Sample name	Conductivity x 10^{-2} S cm^{-1}
PANI	86.15
TP	5.89
CTP	1.85

between TiO_2 and PANI achieved at low loadings. However, a wide study in this regard is essential to explain the exact cause. Clay-Titania-PANI (CTP) composites exhibited activity close to the TP composite. In these composites also, an increase in degradation activity was observed with an increasing of PANI content.

The mechanism and trend of photocatalytic degradation of Acid Orange was found to be the same as in the case of Acid Blue-25. Almost similar activity was observed for the titania composites. Clay composite showed a lesser activity as compared to pure composite at low PANI concentration. An increase in polyaniline content resulted in an increase in activity.

Considerable enhancement in activity was observed for the titania polyaniline composites as compared to pure titania for the degradation of acid orange and acid blue. This suggests efficient shifting of the photoresponse of titania to visible range after polyaniline incorporation. A lowering of activity observed in the case of clay-titania polyaniline composites may be attributed to the lower effective Titania/PANI content.

The high activity of pure titania for methylene blue degradation under visible light may be explained on the basis of dye sensitization mechanism. The main requirement of light induced dye degradation using a catalyst is that the dye must adsorb on the surface of the catalyst. Under visible light illumination, the semiconductor is not excited as its absorption threshold is 385 nm; only the chemisorbed dye is excited at a longer wavelength to produce excited dye species. Subsequently the excited dye injects an electron in to the conduction band of the semiconductor with, the dye being converted to the cation radical. Oxygen plays an important role in scavenging the electron; it suppresses recombination between dye cation radical and e^-. The radical cation ultimately reacts with reactive oxygen radicals and/or molecular oxygen to yield intermediate products or radical species, for which if secondary radical processes occurred might lead to mineralization [32].

However, the activities of titania composites were slightly lowered as compared to pure titania. This may be explained taking into consideration the fact that methylene blue is a cationic dye. The PANI composite is reported to have little affinity towards cationic dyes. The relatively small adsorption of cationic dyes on PANI composite may be due to the repulsive interaction between the positively charged PANI back bone and the cationic part of the dye [33]. Incorporation of PANI resulted in a lowering of the percentage degradation in simple titania as well as clay composites.

The % adsorption of each dye of the catalyst surface was measured by stirring the dye solution with a definite amount of catalyst for a fixed time without irradiation. Also the effects of light on dyes were examined by irradiating the dye solution without catalyst. The results are represented in Table 5. It was found that light without catalyst has no major influence on dye degradation.

A possible mechanism for dye degradation using polyaniline sensitized TiO_2 can be represented as follows (Figure 7). Upon visible light irradiation PANI absorbs visible light to induce π- π* transition. The d-orbital (Conduction Band) of TiO_2 and the π*-orbital of PANI match well in energy level and as a result the excited state electrons of PANI are transported into the d-orbital of TiO_2. These are subsequently transfer to the surface to react with water and oxygen to yield hydroxyl and su-

Table 4. Reactivity Studies

Sample	% degradation		
	Acid blue 25 [a]	**Acid Orange 7** [b]	**Methylene blue** [c]
TiO_2	56	73	97
TP	92	95	93
CTP	59	78	91

a- Catalyst amount = 0.005 g; Irradiation time = 1/2 hour; Lamp Intensity = 150 W; Concentration of dye solution = 10^{-4} M

b - Catalyst amount = 0.005 g; Irradiation time = 45 minutes; Lamp Intensity = 150 W; Concentration of dye = 10^{-4} M

c - Catalyst amount = 0.01 g; Irradiation time = 1 hour; Lamp Intensity = 150 W; Concentration of dye= 10^{-4} M

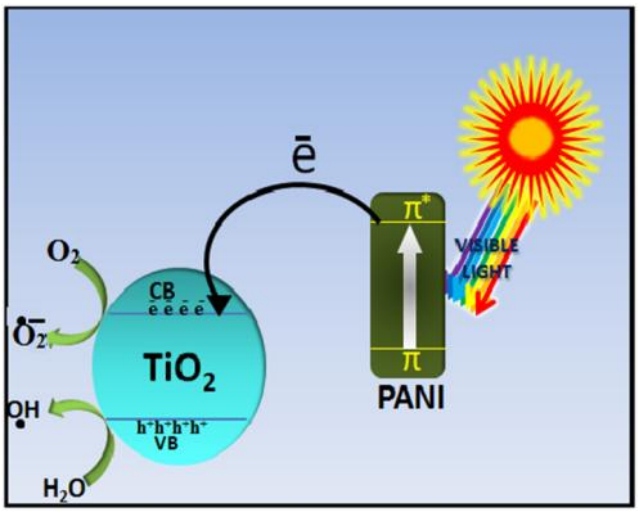

Figure 7. Mechanism of Photocatalytic degradation of dyes using TiO_2 –PANI composite

Table 5. % Adsorption of dyes on catalyst, effect of visible light irradiation on dyes without catalyst and the photocatalytic degradation

Catalysts	Dye	Adsorption %	Light effect	Degradation %
TP	Acid blue	40	1%	99
CTP		50		96
TP	Methylene blue	4.5	2%	78
CTP		10		68
TP	Acid orange	50	4%	98
CTP		65		92

peroxide radicals, which would oxidize or degrade the dye molecules.

5. Conclusions

Different compositions of Titania PANI and Clay Titania PANI composites were prepared and characterized. The photocatalytic activity of these composites was examined by degrading different classes of dyes under visible light. Finally it was concluded that the prepared composites were good photocatalyst under visible light irradiation and also adsorption of dyes on catalyst surface play an important role in the degradation of dyes.

Acknowledgement

Sandhya, K.P. thanks to CSIR, New Dehli for Junior Research Fellowship. Suja Haridas acknowledge to UGC for Financial Support.

References

[1] Liu, G., Li, X., Zhao, J., Hidaka, H., Serpone, N. (2000). Photooxidation pathway of sulforhodamine-B- Dependence on the adsorption mode on TiO_2 exposed to visible light radiation. *Environ. Sci. Technol.* 34: 3982-3990.

[2] Baughman, G.L., Weber, E.J. (1994). Transformation of dyes and related compounds in anoxic sediment: kinetics and products. *Environ. Sci. Technol.* 28: 267-276.

[3] Qin, J., Zhang, Q., Chuang, K.T. (2001). Catalytic wet oxidation of p-chlorophenol over supported noble metal catalysts. *Appl. Catal. B: Environ*. 29: 115-123.

[4] Fujitani, T., Nakamura, J. (2000). The chemical modification seen in the Cu/ZnO methanol synthesis catalysts. *Appl. Catal. A: Gen.* 191: 111-129.

[5] Fox, M.A., Dulay, M.T. (1993). Heterogeneous photocatalysis. *Chem. Rev*. 93: 341-357.

[6] Hoffmann, M.R., Martin, S.T., Choi, W., Bahnemann, D.W. (1995). Environmental Applications of Semiconductor Photocatalysis. *Chem. Rev.*, 95: 69-96.

[7] Linsebigler, A.L., Lu, G., Yates, J.T. (1995). Photocatalysis on TiOn Surfaces: Principles, Mechanisms, and Selected Results. *Chem. Rev*. 95: 735-758.

[8] Wold, A. (1993). Photocatalytic Properties of TiO_2. *Chem. Mater*. 5: 280-283.

[9] Chen, C.C., Li, X.Z., Ma, W.H., Zhao, J.C., Hidaka, H., Serpone, N. (2002). Effect of Transition Metal Ions on the TiO_2-Assisted Photodegradation of Dyes under Visible Irradiation: A Probe for the Interfacial Electron Transfer Process and Reaction Mechanism. *J. Phys. Chem. B* 106: 318-324.

[10] Asahi, R., Morikawa, T., Ohwaki, T., Aoki, K., Taga, Y. (2001). Visible-Light Photocatalysis in Nitrogen-Doped Titanium Oxides. *Science* 293: 269-271.

[11] Wu, G.S., Nishikawa, T., Ohtani, B., Chen, A.C. (2007). Synthesis and Characterization of Carbon-Doped TiO_2 Nanostructures with Enhanced Visible Light Response. *Chem. Mater*. 19: 4530-4537.

[12] Lu, N., Quan, X., Li, J.Y., Chen, S., Yu, H.T., Chen, G.H. (2007). Fabrication of Boron-Doped TiO_2 Nanotube Array Electrode and Investigation of Its Photoelectrochemical Capability. *J. Phys. Chem. C* 111: 11836-11842.

[13] Li, X.Z., Li, F.B. (2001). Study of Au/Au^{3+}-TiO_2 Photocatalysis toward Visible Photooxidation for Water and Wastewater Treatment. *Environ. Sci. Technol*. 35: 2381-2387.

[14] Li, G.S., Zhang, D.Q., Yu, J.C. (2009). A New Visible-Light Photocatalyst: CdS Quantum Dots Embedded Mesoporous TiO_2, *Environ. Sci. Technol*. 43: 7079-7085.

[15] Zhao, W., Sun, Y., Castellano, F.N. (2008) Visible-light induced water detoxification catalyzed by Pt(II) dye sensitized titania, *J. Am. Chem. Soc*. 130: 12566-12567.

[16] Sun, Q., Xu, Y. (2009). Sensitization of TiO_2 with Aluminum Phthalocyanine: Factors Influencing the Efficiency for Chlorophenol Degradation in Water under Visible Light. *J. Phys. Chem. C* 113: 12387-12394.

[17] Yu, G., Gao, J., Hummelen, J.C., Wudl, F., Heeger, A.J. (1995). Polymer Photovoltaic Cells: Enhanced Efficiencies via a Network of Internal Donor-Acceptor Heterojunctions. *Science* 270: 1789-1791.

[18] Zhu, S., Xu, T., Fu, H., Zhao, J., Zhu, Y. (2007). Synergetic effect of Bi_2WO_6 photocatalyst with C60 and enhanced photoactivity under visible irradiation. *Environ. Sci. Technol*. 41: 6234-6239.

[19] Liang, H.C., Li, X.Z. (2009).Visible-induced photocatalytic reactivity of polymer–sensitized titania nanotube films. *Appl. Catal. B: Environ*. 86: 8-17.

[20] Wang, D.S., Zhang, J., Luo, Q.Z., Li, X.Y., Duan , Y.D. (2009). Characterization and photocatalytic activity of poly(3hexylthiophene)-modifiedTiO_2 for degradation of methyl orange under visible light. *J. Hazard. Mater*. 169: 546-550.

[21] Salem, M.A., Al-Ghonemiy, A.F., Zaki, A.B. (2009). Photocatalytic degradation of Allura red and Quinoline yellow with Polyaniline/TiO_2 Nanocomposite. *Appl. Catal. B: Environ*. 91: 59-66

[22] Zhu, Y., Xu, S., Yi, D. (2010). Photocatalytic degradation of methyl orange using polythiophene/titanium dioxide composites: *Reactive & Functional Polymers* 70: 282–287

[23] Gu, L., Wang, J., Qi, R., Wang, X., Xu, P., Han, X. (2012). A novel incorporating style of polyaniline/TiO_2 composites as effective visible Photocatalysts. *J. Molec. Catal. A: Chem*. 357: 19–25

[24] Zhang, G.K., Ding, X.M., He, F.S., Yu, X.Y., Zhou, J., Hu, Y.J., Xie, J.W. (2008). Low-Temperature Synthesis and Photocatalytic Activity of TiO_2 Pillared Montmorillonite. *Langmuir* 24: 1026-1030

[25] Anuar, K., Murali, S., Fariz, A., Mahmud, H.N.M. (2004). Conducting Polymer / Clay Composites: Preparation and Characterization *Materials Science*, 10: 255-258.

[26] Zhang, L., Liu, P., Su, Z. (2006). Preparation of PANI–TiO_2 nanocomposites and their solid-phase photocatalytic degradation. *Polymer Degradation and Stability* 91: 2213-2219.

[27] Ganeshan, R., Gedanken, A. (2008). Organic–inorganic hybrid materials based on polyaniline/TiO_2 nanocomposites for ascorbic acid fuel cell systems. *Nanotechnology* 19: 1-5

[28] Li, X.W., Chen, W., Bian, C.Q., He, J., Xu, N., Xue, G. (2003). Surface modification of TiO_2 nanoparticles by polyaniline. *Appl. Surf. Sci*. 217: 16-22.

[29] Ohtani, B., Ogawa, Y., Nishimotto, S. (1997). Photocatalytic Activity of Amorphous−Anatase Mixture of Titanium(IV) Oxide Particles Suspended in Aqueous Solutions. *J. Phys. Chem*. 101: 3746-3752.

[30] Zhang, Y.X., Li, G.H., Wu, Y.C., Xie, T. (2005). Sol-gel synthesis of titania hollow spheres. *Mater. Res. Bull*. 40: 1993-1999.

[31] Danielle, C.S., Michelle, S.M., Ivo, A.H., Aldo, J.G.Z. (2003). Preparation and Characterization of Novel Hybrid Materials Formed from $(Ti,Sn)O_2$ Nanoparticles and Polyaniline. *Chem. Mater*. 15(24): 4658-4665.

[32] Zhao, J., Chen, C., Ma, W. (2005). Photocatalytic degradation of organic pollutants under visible light irradiation. *Topics in Catalysis*. 35: 269-278

[33] Mahanta, D., Madras, G., Radhakrishnan, S., Patil, S. (2008). Adsorption of sulfonated dyes by polyaniline emeraldine salt and its kinetics. *J. Phys. Chem. B* 112: 10153-1015